

PETROLOGY AND COOLING HISTORY OF MONZOGABBRO SAMPLE 14161,7373:

I. S. MCCALLUM and J.M. SCHWARTZ, Dept. of Geological Sciences, Univ. of Washington, Seattle, WA 98195,
B. L. JOLLIFF and C. FLOSS, Dept. of Earth and Planetary Sciences, Washington Univ., St. Louis, MO 63130

Introduction. Although evolved lithologies are rare among lunar samples, they have assumed a disproportionate importance because they are the products of extensive differentiation processes that occurred early in lunar history and, as such, they provide critical evidence on the magmatic processes that shaped the early Moon. The most common evolved lithologies are the rocks known as quartz monzodiorite (QMD) and granite (felsite). Silicate liquid immiscibility (SLI) has been proposed as a process that produced QMD and granite as conjugate immiscible pairs [1]. Textures reflecting SLI have been produced experimentally in KREEP-like compositions at pressures up to 3 kb [2] but only one sample, 14161,7373, shows clear petrographic evidence for SLI in a plutonic assemblage. In an attempt to constrain the depth of crystallization and immiscible melt formation, we have determined a cooling history based on modeling detailed compositional profiles of exsolved pyroxenes.

Sample Description. Sample 14161,7373 is a small fragment of a monomict whitlockite monzogabbro described initially by Jolliff [3]. Although the rock has been mildly shocked and fractured, it is relatively coarse-grained (by lunar standards) and it has retained relict igneous textures (Fig. 1d). Pigeonite (Fig. 1a), augite (Fig. 1b), plagioclase, and whitlockite form cumulus grains up to 500 microns while these same minerals plus Ba-rich K-feldspar, silica (in a variety of forms), apatite, ilmenite, zircon and troilite make up the intercumulus assemblage. A remarkable feature of this rocklet is the occurrence of egg-shaped micrographic intergrowths of K-feldspar and silica up to 300 microns with interstitial phases molded around the egg (Fig. 1c). 14161,7373 contains a high proportion of whitlockite and can be considered a whitlockite cumulate. The whole-rock rare earth element abundances are the highest of any polymineralline lunar assemblage reported to date (~5-6 x high-K KREEP) [4].

Cooling Rate Determinations. Cooling rates and thermal histories were computed from models of pyroxene exsolution using the method developed by McCallum and O'Brien [5]. The dominant pyroxene is pigeonite which contains (001) lamellae of augite up to 10 μm wide (Fig. 1a). Augite with (001) lamellae of pigeonite (up to 3 μm wide) are less abundant (Fig. 1b). The exsolution lamellae are unusual in that they extend to the edge of the pyroxene grains (Fig. 1a) with no change in thickness suggesting that, after initial crystallization and cooling, the grains were broken and reassembled with some mechanical or chemical abrasion. Many of the fractures in pyroxenes have been healed by veins of troilite \pm silica \pm ilmenite. The veins, which are clearly post-exsolution, are restricted to pyroxenes and whitlockites indicating that this rock has had a complex multi-stage history despite its overall igneous-like texture.

Bulk compositions of pyroxenes and compositions of host—lamellae pairs are shown in Fig. 2. Compositional profiles were determined by a beam scanning technique described by [5]. Areas were scanned for

periods of up to 24 hours—the areas scanned appear as darkened squares in Figs. 1 a and b. The advantage of this method is that it provides a much larger data base which greatly improves deconvolution calculations required to correct for electron beam overlap effects. As shown in Fig. 3, in which a measured and deconvolved profile are compared, the effects of spatial averaging are significant and must be accounted for.

Computation of cooling rates and depth of burial from the deconvolved profiles follows the method of [5]. Figure 4 shows a calculated profile, based on a cooling rate of 8×10^{-3} degrees per year, superimposed on the deconvolved profile. The fit is not perfect but the calculated profile provides a good fit to the lamella width, the compositions of the host and lamella, and the measured profile a few microns removed from the interface. It is impossible to calculate a profile using a *single* cooling rate that simultaneously fits the main part of the profile and the compositional variations in the vicinity of the interface. A cooling rate of 8×10^{-3} degrees per year would correspond to a depth of burial of 950 meters. We interpret these results to indicate that the pyroxene initially crystallized in a fractionated magma of KREEP composition in a chamber at a depth of around 1 km.

Figure 5 shows a calculated profile superimposed on the measured/deconvolved profile in the vicinity of the host—lamella interface. Simulation of this profile requires reheating of the pyroxene for a short period of time to 980°C followed by a period of rapid cooling (2.2 degrees per year) to a closure temperature of around 850°C corresponding to a depth of burial of around 50 meters. Although the fit is not perfect, the cooling rate is well constrained by the location of the minimum in the measured (deconvolved) profile.

Discussion. Pyroxene textures and compositions reflect a complex crystallization and recrystallization history. Our preferred petrogenetic model is based on cooling rate studies and determinations of trace element abundances in individual minerals [4]. Crystallization was initiated at ~1100°C in a KREEP pluton at a depth of around 1 km. Relatively slow cooling resulted in the crystallization of two pyroxenes, plagioclase and whitlockite and the formation of a micro-cumulate texture. Co-crystallization of whitlockite and pyroxene is indicated by a depletion in MREE in pyroxenes. With continued slow cooling, exsolution textures developed in pyroxenes. The onset of silicate liquid immiscibility most likely began near the end of this stage of cooling. Prior to pigeonite inversion, the crystal—melt system was disrupted and transported closer to the surface. Whether this was due to impact is uncertain although this seems likely since the pyroxenes were fractured and suffered mechanical and/or chemical erosion. The ovoid granophyric intergrowths, however, have largely retained their integrity suggesting that they solidified after this event. Relocation close to the surface was accompanied by impact-induced reheating, minor recrystallization and the formation of troilite veins. The bulk composition of 14161,7373 lies near the plagi-

THERMAL HISTORY OF MONZOGABBRO 14161,7373: McCallum, I. S. et al.

clase—pyroxene join in the pseudo ternary system but well removed from the pseudo-ternary cotectic indicating that part of the immiscible felsic melt fraction was lost during the impact event. Finally, a period of rapid cooling followed, most likely insulated by a thin ejecta blanket.

References: [1] Neal and Taylor (1991) *GCA*, 55, 2965. [2] Rutherford et al. (1996) *LPS* XXVII, 1113. [3] Jolliff (1991) *PLPSC*, 21, 101. [4] Jolliff et al. *Amer. Miner.*, submitted. [5] McCallum and O'Brien (1966) *Amer. Miner.*, 81, 1166. [6] Sack and Ghiorso (1994) *CMP*, 116, 287.

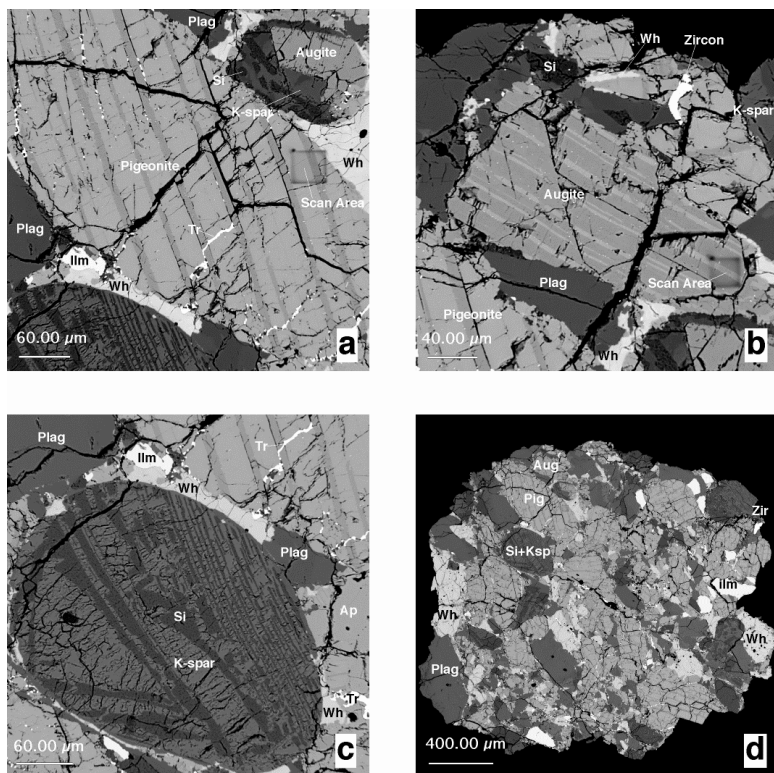


Fig. 1. Back scattered electron images of 14161,7373. (a) Pigeonite with (001) augite lamellae. Note that augite lamellae extend to edge of grain. (b) Augite with (001) pigeonite lamellae. (c) Egg-shaped granophyric intergrowth [K-spar + silica] formed by silicate liquid immiscibility. Note the phases molded around the egg. (d) Whole rock showing the microcumulate texture, the high mafic content, and the immiscible granitic blebs.

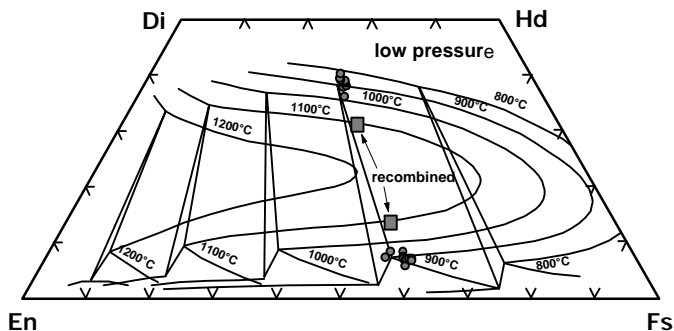


Fig. 2. Pyroxene compositions in 14161, 7373. Bulk compositions are shown by squares, host-lamella compositions are shown as circles. Solvus isotherms after Sack and Ghiorso (1994) are projected on to the quadrilateral.

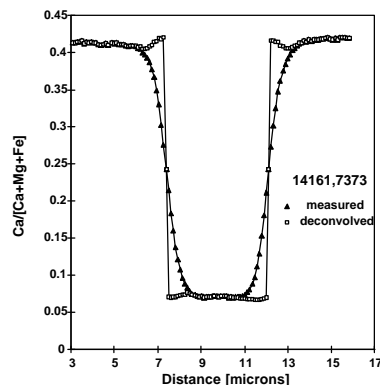


Fig.3 Measured and deconvolved profiles in augite. Note the minimum in $Ca/[Ca+Mg+Fe] \sim 1 \mu m$ from interface.

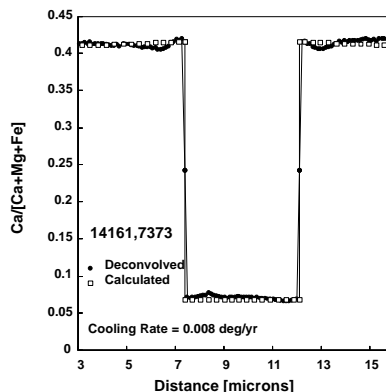


Fig. 4. Best fit calculated profile [cooling rate = 0.008°C/year] superimposed on the deconvolved profile.

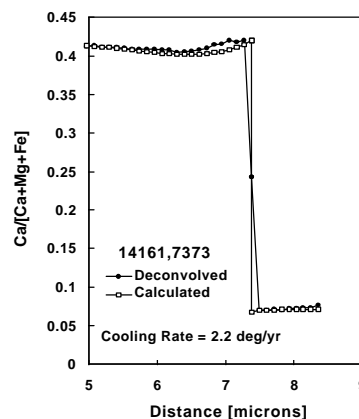


Fig. 5. Calculated profile in vicinity of host-lamella interface.